Steady State Simulation and Exergy Analysis of Supercritical Coal-fired Power Plant with CO_2 Capture

Akeem K Olaleye[1], Meihong Wang*[,1], Greg Kelsall[2]

[1]*Process and Energy Systems Engineering Group, School of Engineering, University of Hull, Cottingham Road, Hull, United Kingdom, HU6 7RX*

[2]*Alstom Power, Newbold Road, Rugby, CV21 2NH Warwick, United Kingdom*

Abstract

Integrating a power plant with CO_2 capture incurs serious efficiency and energy penalty due to use of energy for solvent regeneration in the capture process. Reducing the exergy destruction and losses associated with the power plant systems can improve the rational efficiency of the system and thereby reducing energy penalties. This paper presents steady state simulation and exergy analysis of Supercritical coal-fired power plant (SCPP) integrated with post-combustion CO_2 capture. The simulation was validated by comparing the results with a greenfield design case study based on a 550 MW_e SCPP unit. The analyses show that the once-through boiler exhibits the highest exergy destruction but also has a limited influence on fuel-saving potentials of the system. The turbine subsystems show lower exergy destruction compared to the boiler subsystem but more significance in fuel-saving potentials of the system. Four cases of the integrated SCPP-CO_2 capture configuration was considered for reducing thermodynamic irreversibilities in the system by reducing the driving forces responsible for the CO_2 capture process: conventional process, absorber intercooling (AIC), split-flow (SF), and a combination of absorber intercooling and split-flow (AIC+SF). The AIC+SF configuration shows the most significant reduction in exergy destruction when compared to the SCPP system with conventional CO_2 capture. This study show that improvement in turbine performance design and the driving forces responsible for CO_2 capture (without compromising cost) can help improve the rational efficiency of the integrated system.

Keywords: Post-combustion carbon capture; Supercritical coal-fired power plants; Conventional Exergy Analysis; Advanced Exergy Analysis; Steady state process simulation

Nomenclature

Symbol	Description	Units
$\dot{\boldsymbol{E}}_{\boldsymbol{n}}$	Exergy of component n	MW
$\dot{\boldsymbol{E}}_{\boldsymbol{F,n}}$	Fuel Exergy of component *n*	MW
$\dot{\boldsymbol{E}}_{\boldsymbol{P,n}}$	Product Exergy of component *n*	MW
$\dot{\boldsymbol{E}}_{\boldsymbol{D,n}}$	Exergy destruction of component *n*	MW
$\dot{\boldsymbol{E}}_{\boldsymbol{D,n}}^{\boldsymbol{un}}$	Unavoidable exergy destruction of *n*	MW
$\dot{\boldsymbol{E}}_{\boldsymbol{D,n}}^{\boldsymbol{av}}$	Avoidable exergy destruction of *n*	MW
$\dot{\boldsymbol{E}}_{\boldsymbol{D,n}}^{\boldsymbol{en}}$	Endogenous exergy destruction of *n*	MW
$\dot{\boldsymbol{E}}_{\boldsymbol{D,n}}^{\boldsymbol{ex}}$	Exogenous exergy destruction of *n*	MW
$\dot{\boldsymbol{E}}_{\boldsymbol{D,n}}^{\boldsymbol{av,ex}}$	Avoidable exogenous exergy destruction of *n*	MW
$\dot{\boldsymbol{E}}_{\boldsymbol{D,n}}^{\boldsymbol{un,ex}}$	Unavoidable exogenous exergy destruction of *n*	MW
$\dot{\boldsymbol{E}}_{\boldsymbol{D,n}}^{\boldsymbol{av,en}}$	Avoidable endogenous exergy destruction of *n*	MW
$\dot{\boldsymbol{E}}_{\boldsymbol{D,n}}^{\boldsymbol{un,en}}$	Unavoidable endogenous exergy destruction of *n*	MW
$\Delta \boldsymbol{E}^{*,\boldsymbol{n}}$	Fuel saving potential	MW
$\boldsymbol{\Delta T}$	Temperature difference	^{o}C
$\boldsymbol{y}$	Exergy loss ratio	-
$\boldsymbol{Q}$	Heat flow	J/s
Greek Symbol		
α	Air fuel ratio	-
η	Boiler efficiency	%
$\dot{\boldsymbol{\varepsilon}}$	Exergetic efficiency	%
Subscript		
n	component	
max	maximum	
F	Fuel	
L	Loss	
min	minimum	
P	product	
isent	isentropic	
Acronyms		
SCPP	Supercritical Coal-fired Power Plant	
AIC	Absorber Inter-Cooling	
SF	Split-Flow	
IAPWS	International Association for the Properties of water and steam	
R	Real	
U	Unavoidable	
FGD	Flue gas desulphurization	
HHV	High heating value	
SSH	Secondary superheater	
FWH	Feedwater heater	
RHT	Reheater	
TH	Theoretical	
GPDC	Generalized pressure drop correlation	

1 Introduction

1.1 Background

Coal-fired power plants play a vital role in meeting energy demands. However, power generation from coal-fired power plants is the single largest source of CO_2 emissions. CO_2 is the largest and most important anthropogenic greenhouse gas (GHG) [1]. With growing concerns over the increasing atmospheric concentration of anthropogenic greenhouse gases, effective CO_2 emission abatement strategies such as power plant efficiency improvement, carbon capture and storage (CCS) are required to combat this trend [2].

An integration of high efficient coal-fired power plant with CO_2 capture will further lead to a better management of this challenge since every increment in efficiency results in a reduction in CO_2 emission per MW electricity generated. The supercritical coal-fired power plant (e.g. ultra-supercritical) for its very high efficiency (between 45 – 50 % LHV) [3] coupled with CO_2 capture plant have been identified as the best solution to synergistically deal with threat of climate change and increase in energy demand. However, integrating a power plant with CO_2 capture incurs serious energy penalty due to the energy use for solvent regeneration in the capture process and subsequent increase in cost of electricity [4].

Reducing the losses associated with the power plant systems is another way of improving the system efficiency and thereby reducing cost. This will give insights into individual system behaviours and aid the design of systems by helping to identify locations and magnitudes of wastage, losses, and to evaluate the meaningful efficiency of the system [5]. Conventional power plant efficiency assessment based on energy analysis is only quantitative (first law of thermodynamics) but not qualitative. However, Exergy analysis assesses the energy quantitatively and qualitatively.

1.2 *Review of Exergy analysis of thermal power plant and CO_2 Capture*

Exergy analysis of thermal power plants has been investigated by a number of researchers since the early 1980s and has been widely applied to different configurations of thermal power plants [3]. Some of the researchers have focused on energy and exergy analyses of subcritical, supercritical (SCPP) and ultra-supercritical (Ultra-SCPP) steam power plants [3, 5-10] while some have extended the analyses to include varying load conditions [5, 11] and efficient design of power plant components by exergy loss minimization [12]. A large number of studies have also considered combined cycle gas turbine (CCGT) power plants investigating different components exergy losses [13-15]. Exergy analysis of standalone (pre-combustion or post-combustion) CO_2 capture plants [16-18] have also been carried out to investigate the effects on the associated penalties and power plants efficiency reduction. Analysis of CO_2 capture plant integrated to a power plant has also been investigated. Most of the integrated SCPP processes have focused mainly on energetic analysis [19-24], while few have included exergy analysis while investigating the improvement of efficiency of power plant with CO_2 capture [25-27].

With the widespread progress of SCPP and the ultra-SCPP due to its higher efficiency and lower emission per MWe generated, and the further improvement in its potential through CO_2 capture integration, an investigation of efficiency improvement is very important. Exergy analysis will

identify the losses associated with this integrated systems, investigate strategies for improvement, and also reduce the penalties due to the capture process.

1.3 Aim of this paper and its Novel Contribution

Exergetic investigation on SCPP and Ultra-SCPP concepts has already been performed [3, 10]. However, a detailed exergetic analysis of the complex process to analyse where and why the losses occur in SCPP with CO_2 capture is lacking. Therefore this paper focuses on the exergy loss analysis of entire SCPP with CO_2 capture and strategies to reduce these losses. This study include (i) steady state simulation of SCPP and post-combustion CO_2 capture (ii) conventional and advanced exergy analysis of SCPP with CO_2 capture (ii) reduction of exergy destruction and losses in the integrated system.

2 Steady State Simulation of SCPP with CO_2 Capture Plant

2.1 Reference Plant Description

The reference SCPP used in this study is a greenfield power plant of 580 MWe SCPP with flue gas desulphurisation (FGD) and CO_2 capture described in Woods *et al* [28]. The steam turbine conditions correspond to 24.1 MPa/593ºC throttle with 593ºC at the reheater. Net plant power, after consideration of the auxiliary power load is 550 $MW_{e.}$ The plant operates with an estimated efficiency of 39.1 % (HHV). The major subsystems of the plant includes: Coal milling system, coal combustion system, ash handling system, FGD, Condensate and feedwater systems etc. The key design parameters are listed in Table 1. Figure 1 shows the hierarchical simulation of the overall flowsheet of the reference plant in Aspen Plus® V8.The Aspen plus simulation is carried out in eight different hierarchies: (i) the coal mill; (ii) the SC-once through boiler; (iii) feedwater heaters and steam extractions; (iv) steam turbines; (v) condenser and hotwell; (vi) flue gas desulfurization; (vii) air preheating; (viii) the post-combustion CO_2 capture. The reference SCPP consists of eight feedwater heaters (including the deaerator); seven were modelled as heat exchangers while the deaerator was modelled as a mixer. The feedwater from the deaerator is pumped into the boiler through a boiler feed pump (turbine driven).

Table 1 Key parameters of the SCPP unit [28]

Description	Value
Steam cycle (MPa/ºC/ºC)	24.1/593/593
As received coal (kg/hr)	186,555
Coal Heating Value, HHV (MJ/kg)	27.113
Condenser pressure (mmHg)	50.8
Boiler Efficiency (%)	89.0
Cooling water to condenser (ºC)	16.0
Cooling water from condenser (ºC)	27.0
HP Turbine efficiency (%)	90.0
IP Turbine efficiency (%)	92.0
LP Turbine efficiency (%)	94.0
Generator efficiency (%)	98.4
Excess air (%)	20.0
Stack temperature (ºC)	57.0
FGD Efficiency (%)	98.0

Fabric filter efficiency (%)	99.8
Ash Distribution, Fly/Bottom ash	80%/20%

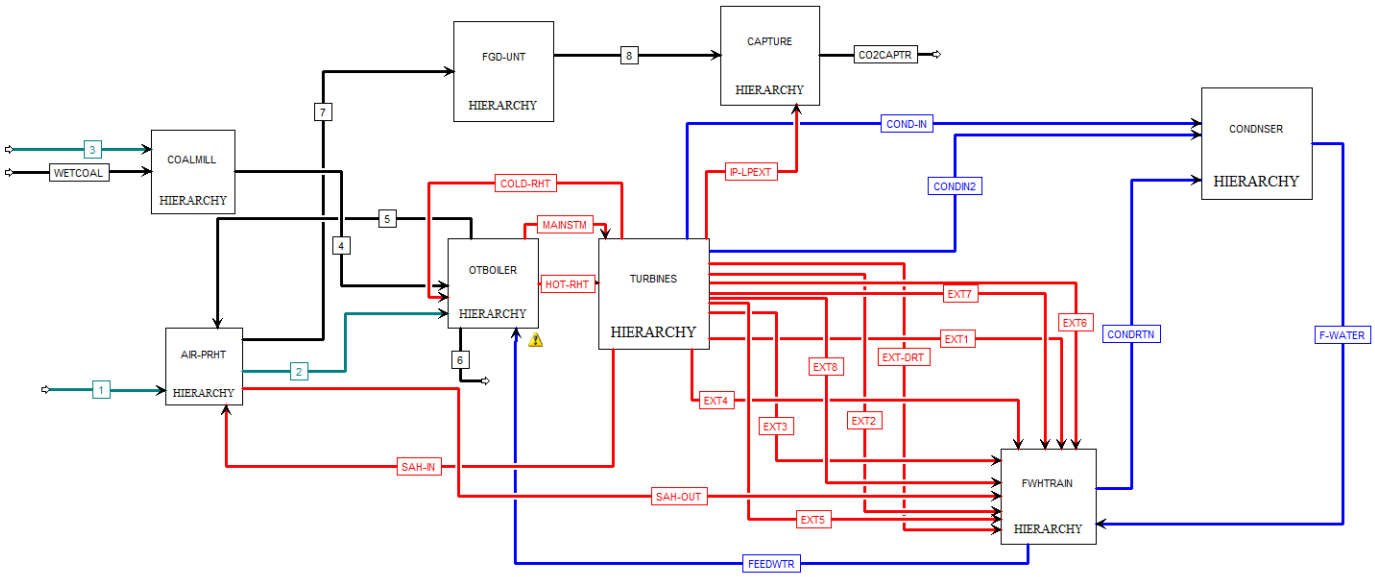

Figure 1: Hierarchical model of SCPP with CO_2 capture in Aspen Plus®

2.2 SCPP Simulation – Reference Case

Simulation of the SCPP system and the CO_2 capture process requires the thermodynamic properties of the systems components to be properly defined for accurate representation of the reference case. Aspen plus® simulation of the SCPP uses the MIXNCPSD stream class which takes into account the particle size distribution for the coal pulveriser, non-conventional substances (i.e. ash and coal), conventional and mixtures (i.e. gases) etc. Four property methods were selected for the simulation of the power plant: Peng Robinson and Boston Mathias (PR-BM) for the estimation of properties of solid, Soave Redlich Kwong (RKS), Electrolyte NRTL for the electrolytes components in the CO_2 capture process, Ideal gas equation for air and flue gases, and the STEAMNBS steam table (which contains the IAPWS-F97 formulation for property of water and steam at supercritical condition) for water and steam.

2.2.1 Once-through boiler subsystem

The once-through boiler consists of the pulverized coal conveyed from the pulverizer subsystems, the burners & furnace, and the heat exchanger units. The heat exchanger units include the primary superheaters (PSH-1 and PSH-2), the secondary superheaters (SSH-1 and SSH-2), the reheater (RHT), and the economisers (ECON). Figure 2 shows the Aspen Plus® model of the once-through boiler with the connection ports to other hierarchies in Figure 1. The flue gas from the boiler goes into flue gas desulphurization unit which consists of a fabric filter and desulphurizer for removal of particulates and sulphur respectively.

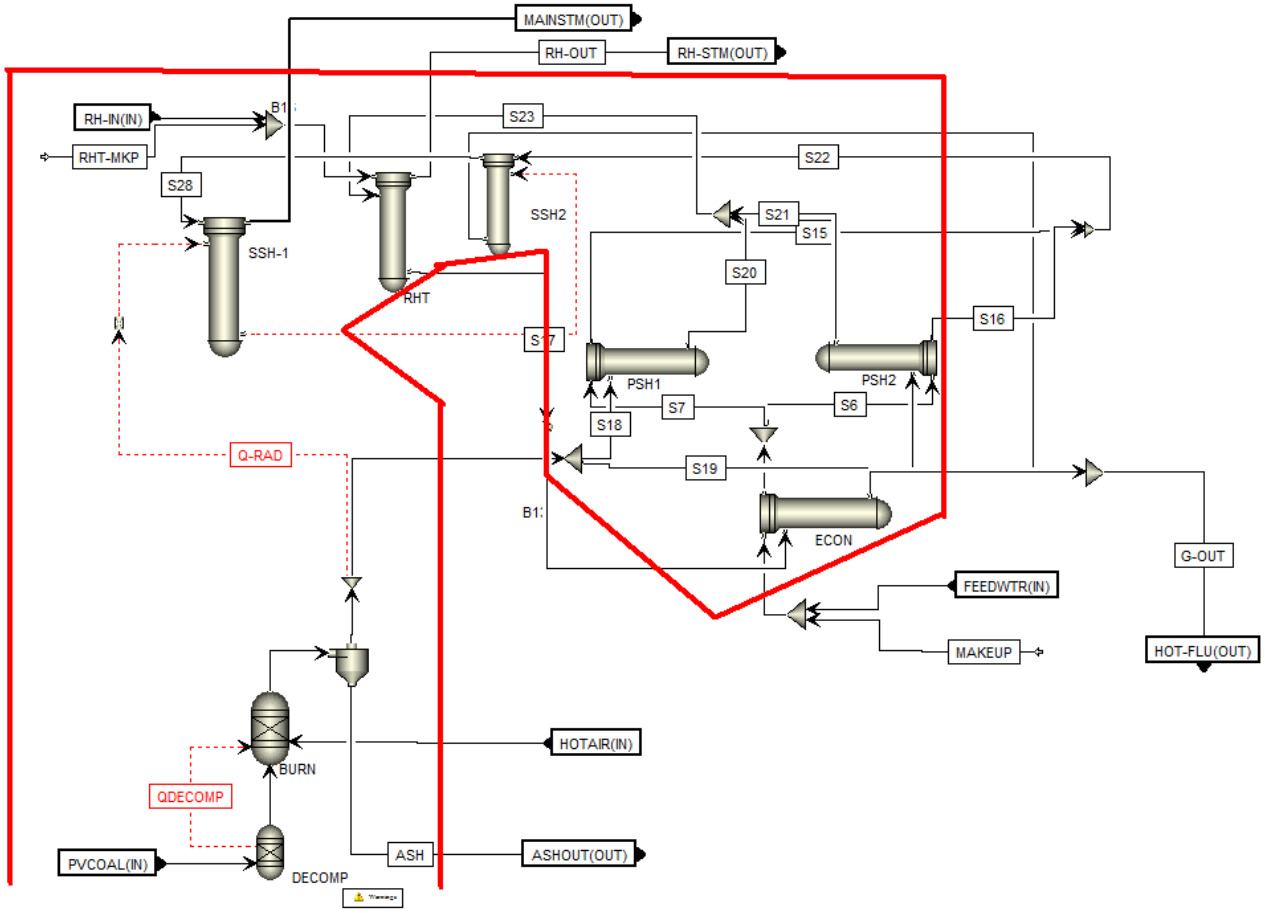

Figure 2: Aspen Plus® simulation of Once-through boiler of SCPP

2.2.2 Steam turbines and steam extraction subsystem

The turbine subsystem of the SCPP is made up of the low-pressure (LP), intermediate-pressure (IP), and the high-pressure (HP) sections. The main steam expands through stages of the VHP-TURB, HP-TURBs, IP-TURBs, and the LP-TURBs (Figure 3) to generate shaft work for electric power. The final exhausted steam at the last stage of the turbine (LP-TURB4) is condensed in a condenser. The turbines also consist of stream extraction ports that connect the extracted steam from the turbines to the feedwater heating train (FWHTRAIN) hierarchy for regenerative feedwater heating; the main steam line from the once-through boiler hierarchy (MAINSTM), and the reheat steam lines (RH-STM and RH-IN).

2.2.3 Feedwater Heating train

As part of efficiency improvement in the SCPP, regenerative feedwater heating is done; using steam extracted from the different points on the turbines to heat the feedwater as shown in Figure 4. The train consists of four high pressure (FWH5 to FWH8) and four low pressure closed feedwater heat exchangers (FWH1 to FWH4); and one open feedwater heat exchanger (i.e. deaerator). The system also includes an extraction point from the boiler feed pump turbine to meet the power requirement of the feed pump.

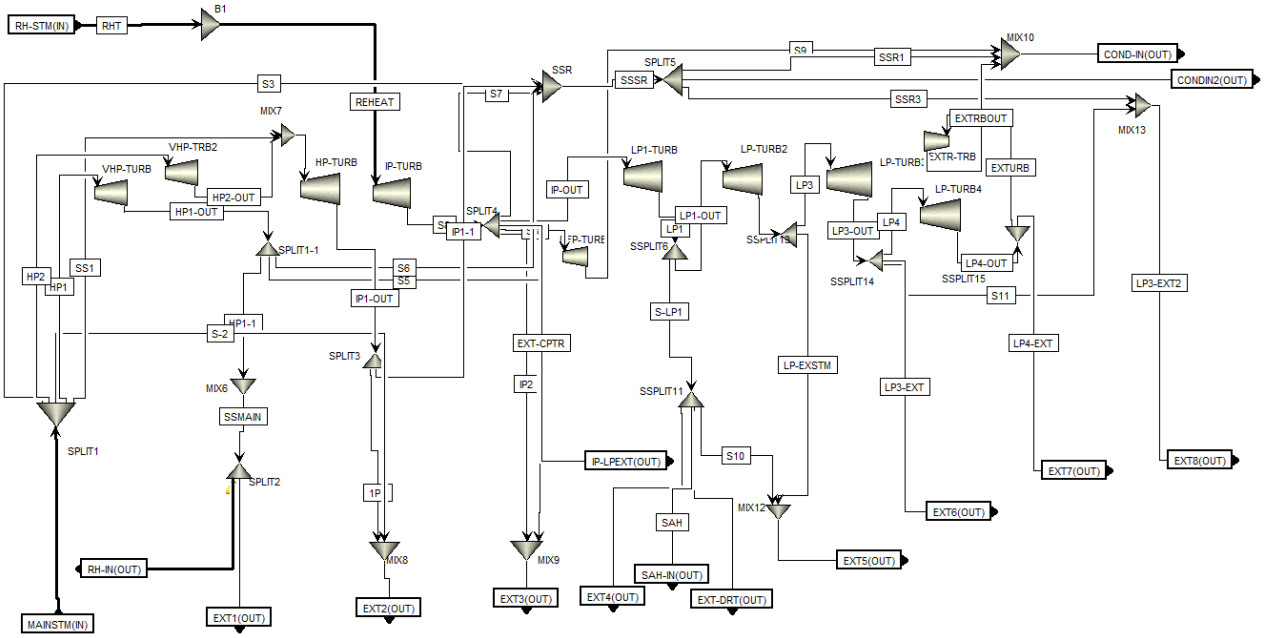

Figure 3: Model of the Turbines and Steam Extraction in Aspen Plus®

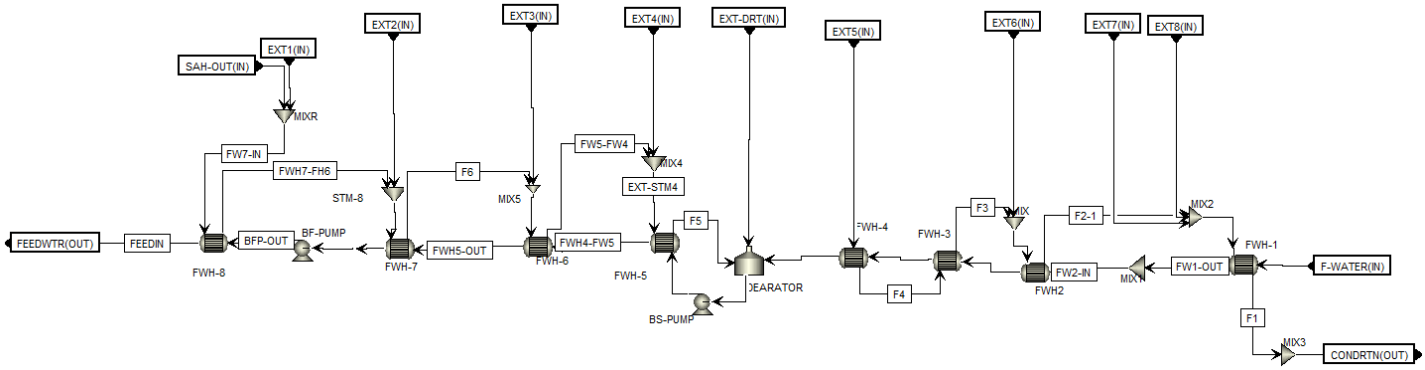

Figure 4: Model of the Feedwater Heating Trains in Aspen Plus®

Table 2 shows the simulation results and validation with the reference plant based on the main stream parameters. Table 3 shows the performance comparison with the reference power plant described in Woods *et al* [28].

2.3 MEA-Based Post-Combustion CO_2 Capture Plant

Post-combustion CO_2 capture (PCC) is one of the strategic technologies identified to reduce emission of greenhouse gases in existing power plant [2]. PCC based on chemical absorption of monoethanolamine (MEA) is the most matured and preferred technology for CO_2 capture from the flue gases in existing power plant. In this study, data from a CO_2 capture pilot facility is used for validation of the model.

Table 2 Validation of SCPP Simulation based on the Main stream Parameters

Main Streams	Reference	Aspen plus®	Rel. error (%)	Reference	Aspen Plus®	Rel. error (%)	Reference	Aspen Plus®	Rel. error (%)
Coal/air/flue gas	Temperature (°C)			Pressure (bar)			Mass Flow (kg/s)		
WET COAL	15.0	15.0	0.0	1.014	1.014	0.0	56.0	56.0	0.0
1	15.4	15.4	0.0	1.014	1.014	0.0	390.0	390.0	0.0
2	235.1	229.7	2.4	1.110	1.130	1.8	390.0	390.0	0.0
3	15.4	15.4	0.0	1.014	1.014	0.0	120.0	120.0	0.0
4	20.0	22.1	0.6	1.110	1.110	0.0	52.0	51.6	0.8
5	368.0	365.2	0.76	0.993	1.005	1.2	570.0	569.5	1.5
6	368.0	365.2	0.83	0.993	1.005	1.2	1.01	1.01	0.0
7	116.0	115.4	0.36	0.979	0.985	0.6	566.0	565.8	1.25
8	57.0	56.8	0.7	1.014	1.013	0.1	605.0	603.4	0.71
Steam/water path									
FEEDWTR	313.0	310.8	0.7	290.0	290.0	0.0	465.0	464.2	0.2
MAINSTM	593.0	591.5	0.3	243.0	242.6	0.2	465.0	464.2	0.2
HOT-RHT	593.0	591.5	0.3	45.0	45.2	0.4	385.0	384.6	0.1
COLD-RHT	352.0	356.0	1.1	49.01	51.0	4.1	385.0	384.6	0.1
CONDRTN	44.8	45.2	0.9	0.3	0.29	1.0	60.0	60.4	0.7
F-WATER	39.2	40.1	2.3	17.0	16.8	1.2	350.0	350.0	0.0

Table 3 SCPP Performance Summary

Performance Parameters	Reference Plant	Aspen Plus®	Rel. error (%)
Total (steam turbine) power output (MWe)	580.26	585.39	0.9
Auxiliary Load (MWe)	28.28	28.42	0.5
Gross plant power(MWe)	551.98	556.97	0.9
Generator Loss (MW)	1.83	1.83	-
Net Power output (MWe)	550.15	555.14	0.9
Unit efficiency, HHV (%)	39.1	39.4	0.78

2.3.1 *Chemistry of the MEA-H_2O-CO_2 System*

The solution chemistry for CO_2 absorption with MEA includes water dissociation, CO_2 hydrolysis, bicarbonate dissociation, carbamate hydrolysis, and MEA protonation [29] thus:

$$2H_2O \leftrightarrow H_3O^+ + OH^- \quad (r1)$$

$$CO_2 + 2H_2O \leftrightarrow HCO_3^- + H_3O^+ \quad (r2)$$

$$HCO_3^- + H_2O \leftrightarrow HCO_3^{2-} + H_3O^+ \quad (r3)$$

$$MEACOO^- + H_2O \leftrightarrow MEA + HCO_3^- \quad (r4)$$

$$MEAH^+ + H_2O \leftrightarrow MEA + H_3O^+ \quad (r5)$$

In addition to the thermodynamic properties, the kinetics for carbamate formation (r6 and r7) were obtained from Hikita et al [30], while the reaction for bicarbonate formation (r8 and r9) are obtained from Pinset et al [31]. Reaction rates are solved by power law expressions in Aspen plus® using the rate expressions and constants obtained from [30] and [31]. The equilibrium reactions (r1 – r5) are modelled using data available in Aspen Plus®.

$$MEA + CO_2 + H_2O \rightarrow MEACOO^- + H_3O^+ \quad (r6)$$

$$MEACOO\text{-} + H_3O^+ \rightarrow MEA + CO_2 + H_2O \quad (r7)$$

$$CO_2 + OH^- \rightarrow HCO_3^- \quad (r8)$$

$$HCO_3^- \rightarrow CO_2 + OH^- \quad (r9)$$

2.3.2 *Simulation of the Rate Based Model*

The MEA-based CO_2 capture developed in this simulation is based on the pilot plant data from University of Kaiserslautern [32]. Model development of the closed-loop CO_2 capture plant (Figure 5) is presented in this study and validated against the pilot plant data in [32] for a rate-based modelling approach. In this model, the liquid phase non-ideality is accounted for with the electrolyte NRTL property method while the vapour phase uses the Redlich-Kwong equation of state. The transport property model parameters for density, viscosity, surface tension, thermal conductivity, and diffusivity presented in Aspen plus® were examined and updated with literature data [33]. The built-in correlations in Aspen Plus® are used to calculate the performance of packing. For the structured packing of BX 500, the 1985 correlations of Bravo et al. [34] are used to predict the mass transfer coefficients and the interfacial area. The 1992 correlation of Bravo et al. [35] is used to calculate the liquid holdup and the Chilton and Colburn correlation [36] is used to calculate the heat transfer coefficients.

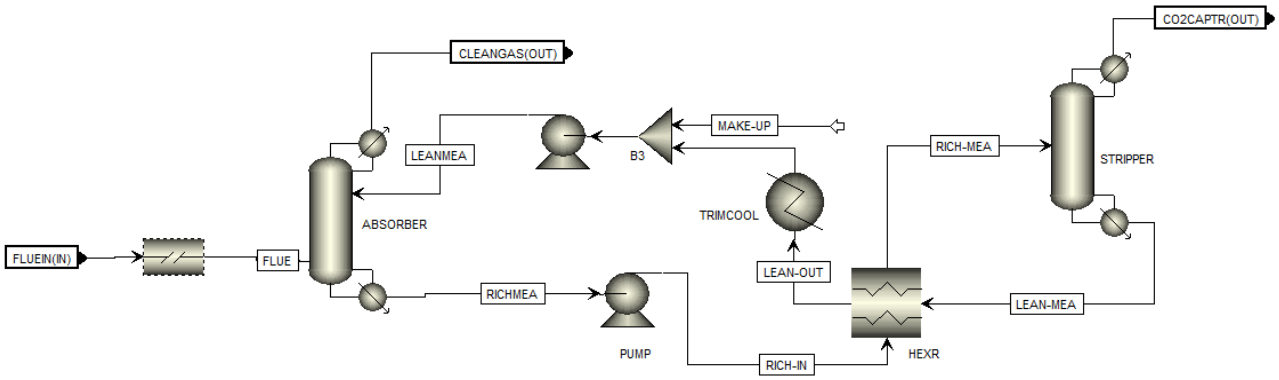

Figure 5: Aspen simulation of conventional MEA-Based PCC

2.3.3 Validation and Scale-up of the Rate-based Model

In the SCPP, the flue gas leaves the desulphurization unit at a temperature of 57^{o}C and is pre-cooled to about 40^{o}C in a direct contact cooler before it enters the absorber. The validated MEA-based PCC is scaled up to handle the flue gas stream from the 550MWe SCPP. The Aspen plus® model was validated with data from the pilot plant. The validated model was scaled-up using Chemical Engineering design principles as described in [37]. The method employed in determining the column diameter and subsequently the column height for both the absorber and the desorber is the generalized pressure drop correlation (GPDC) principle [37, 38]. The capture model originally based on pilot plant data was scaled up to process flue gas from a 550MWe SCPP unit. At full load, the flue gas flowrate of the plant is 603.4 kg/s with 21.35 wt. % of CO_2. Table 4 shows some of the process specifications and preliminary calculation results for the scale-up of the MEA-based PCC plant. The required solvent flow rates are evaluated using the initial estimates based on Table 4 to achieve a CO_2 capture level of 90 wt. % and purity of the CO_2 stream leaving the stripper of 95 wt. %.

Table 4 Design Parameters for the Scale-up of the MEA-based PCC unit

Description	Value
Flue gas mass flow rate (kg/s)	603.4
Flue gas composition (CO_2)	0.2135
Flue gas composition (N_2)	0.7352
Flue gas composition (H_2O)	0.0513
CO_2 Capture level (%)	90.0
Estimated flowrate of CO_2 Capture (kg/s)	128.83
Required MEA flowrate (kg/s)	828.193
Estimated Lean solvent flow rate (kg/s)	2717.168
Estimated Rich solvent flow rate (kg/s)	3040.2
Lean MEA mass fraction (wt. %)	30.48
Lean MEA CO_2 loading (mol CO_2/mol MEA)	0.29

Operation of packed columns are limited by (i) flooding, which occurs when a gas flow pressure drop is so high that the liquid is unable to flow downward and it sets the upper capacity limit of the packed column; and (ii) the minimum liquid load, which is the lowest liquid flowrate that gives sufficient mass transfer rate [38]. An efficient packed column design is characterised by a good liquid and gas distribution that is achieved by operating at the highest economical pressure drop. The pressure drop per metre packing for absorbers and strippers of 1 to 12 mbar/m of packing height is recommended for the Sulzer BX 500 structured packing; typically away from the flooding line [39]. 10.5 mbar/m of packing height was used for the design of both the absorber and stripper [39].

In this study, the Sulzer BX 500 structured packing is selected because of its higher surface area and low regeneration energy at higher CO_2 removal rates when compared with Mellapak 250.Y [32]. Due to structural limitations, column diameters for the structural packing; Sulzer BX 500 should not exceed 6 m (the largest diameter of the packing supplied to date) [39]. Hence, to capture the large volumes of flue gases from the SCPP will require more than one absorber, which could in turn improve the turn down ratio of the process [38]. Therefore, from the cross-sectional areas determined for both the absorber and regenerator, a number of parallel units may be needed to meet

the capacity requirements. The minimum number of the absorbers and the strippers are determined based on the required column capacities [38]. Using one column would result in a diameter of 16.32 m and 13.06 m for the absorber and the stripper respectively, which would be difficult to manage due to structural limitations. Therefore, to process the large volume of flue gas from the SCPP unit, four absorption columns with a diameter of 5.74m and three desorber column of 5.33m diameter are designed for the integrated SCPP process. Table 5 shows a summary of the key variables of the scaled-up MEA-based PCC unit integrated with the SCPP process.

Table 5 Key Process parameters of the PCC model

Parameter	Absorber	Desorber
Calculation type	Rate-based	Rate-based
Type of packing	Sulzer BX 500	Sulzer BX 500
Total Height of Packing (m)	35.0	30.0
Diameter of column (m)	5.74	5.33
Column Number	4	3
No. of Equilibrium stages	30	30
Operating Pressure (bar)	1.013	1.62

3 Exergy Analysis

In this section, conventional and advanced exergy approaches are used to evaluate the exergy destructions and potential for improvement of the SCPP system integrated with CO_2 capture.

3.1 Conventional Exergy Analysis

Exergy defines the maximum possible work potential of a system, a stream of matter and/or heat interaction using the state of the environment as the datum [40]. Conventional exergy analysis identifies the location, magnitude, and sources of thermodynamic inefficiencies in a thermal system.

3.1.1 SCPP Components

Aspen Plus® V8 contains three new property sets; EXERGYMS, EXERGYML (calculated on mass and molar basis respectively), and EXERGYFL for estimating exergy of material/energy streams, unit operation and utilities. These properties are estimated at a reference temperature and pressure [40]. Detailed calculation methods for physical and chemical exergies of the material flows, work, and heat flows for each SCPP components are estimated using the individual stream flow based on the Aspen Plus® EXERGYMS stream calculations.
The following equations are generally used for evaluation of an individual component and the overall system exergy destruction rate within a component.

The exergy balance for the overall SCPP system can be written as [3]

$$\dot{E}_{F,total} = \dot{E}_{P,total} + \dot{E}_{D,total} + \dot{E}_{L,total} = \dot{E}_{P,total} + \sum \dot{E}_{D,n} + \dot{E}_{L,total} \qquad (1)$$

Whereas for the nth component,

$$\dot{E}_{F,n} = \dot{E}_{P,n} + \dot{E}_{D,n} + \dot{E}_{L,n} \qquad (2)$$

The exergy efficiency of the nth component

$$\dot{\varepsilon}_n = \dot{E}_{P,n}/\dot{E}_{F,n} = 1 - \dot{E}_{D,n}/\dot{E}_{F,n} \qquad (3)$$

and the exergy destruction ratio of the n^{th} component

$$y_{D,n} = \dot{E}_{D,n} / \dot{E}_{F,total} \quad (4)$$

for the overall SCPP system, the exergy loss ratio is,

$$y_L = \dot{E}_{L,total} / \dot{E}_{F,total} \quad (5)$$

The chemical exergy of coal is calculated by multiplying its HHV with a constant factor, normally 1.02 [42]. The Aspen Plus® default value of exergy reference environment temperature and pressure of 298.15 K and 1.013 bar was used throughout the simulation.

3.1.2 CO_2 Capture Plant

Thermodynamic reversibility demands that all process driving forces i.e. temperature, pressure and chemical potential differences be zero at all points and times [43]. Such a theoretical process results in the production of the maximal amount of useful work (exergy), or in the consumption of the minimal amount of work. Unfortunately, a reversible chemical process operates at an infinitesimal rate, and requires an infinitely large plant [43]. It has been generally believed that thermodynamic irreversibility in chemical processes/reactions is almost inevitable and leads to large energy consumption and losses [44]. However, some thermodynamic principles based on the second law of thermodynamics such as the so called "counteraction principle", "driving force method", "quasi-static method" etc. have been investigated and proven effective for lowering energy consumption more than often predicted [43]. This study uses the driving force method to reduce exergy destruction and hence reduce energy consumption in MEA-based PCC process without changing the absorbent. Three configurations of the MEA-based PCC were simulated. This includes (i) absorber intercooling (AIC), (ii) split flow approach (SF), and (iii) combination of both methods (AIC+SF).

Aspen plus® exergy estimation property set is used in estimating the exergy of the CO_2 capture unit. However, to determine the exergy of reaction systems involving electrolytes (i.e. reaction of MEA and CO_2), certain adjustment had to be made to the thermodynamic properties of the ionic species of MEA (i.e. $MEAH^+$ and $MEACOO^-$) supplied by the Aspen Plus property databank. Estimation of the mixing exergy is important to accurately estimate the overall exergy destruction in the CO_2 capture system. The Gibbs free energy of formation (DGAQFM) of the ionic species $MEAH^+$ and $MEACOO^-$ which is unavailable in the MEA system databank in Aspen Plus® will have to be estimated. The DGAQFM values used in this study is based on the estimate by [16]. Guezebebroek *et al* [16] used data generated by Aspen Plus® for a mixture of MEA and H_2O to calculate the DGAQFM. The DGAQFM values of -500.504 kJ/mol and -196.524kJ/mol were obtained for $MEAH^+$ and $MEACOO^-$ respectively.

Table 6 shows the computation of the exergy destructions and efficiency for the process equipment in the SCPP subsystems and the conventional MEA-Based PCC systems.

Table 6 Conventional Exergy Analysis of SCPP with CO_2 Capture

Components	$E_{F,n}$(MW)	$E_{P,n}$(MW)	$E_{D,n}$(MW)	$y_{D,n}$(%)	$\mathcal{E}_n$(%)	Components	$E_{F,n}$(MW)	$E_{P,n}$ (MW)	$E_{D,n}$ (MW)	$y_{D,n}$(%)	$\mathcal{E}_n$(%)
Boiler Subsystem						*Feedwater Heating Subsystem*					
COALMILL	1430.61	1425.00	5.61	0.39	99.61	FWH-1	9.96	8.04	1.92	0.13	80.72
AIR-PRHT	81.11	61.67	19.44	1.36	76.03	FWH-2	9.92	6.57	3.35	0.23	66.23
DECOMP	1427.01	1426.85	0.16	0.01	99.99	FWH-3	4.36	3.47	0.89	0.06	79.59
BURN	1487.97	1005.98	481.99	33.69	67.61	FWH-4	16.87	12.85	4.02	0.28	76.17
SSH-1	109.51	83.26	26.25	1.83	76.03	DEAERATOR	22.76	19.31	3.45	0.24	84.84
RHT	41.60	30.10	11.50	0.80	72.36	BS-PUMP	3.50	3.12	0.38	0.03	89.14
SSH2	93.70	72.38	21.32	1.49	77.25	FWH-5	23.18	19.83	3.35	0.23	85.55
PSH1	54.37	45.67	8.70	0.60	84.00	FWH-6	41.69	38.27	3.42	0.24	91.80
PSH2	64.99	52.93	12.06	0.85	81.44	FWH-7	28.79	27.08	1.71	0.12	94.06
ECON	46.58	33.90	12.68	0.89	72.78	FWH-8	20.73	16.81	3.92	0.27	81.09
						BFP	17.84	15.79	2.05	0.14	88.51
Turbine Subsystem						*FGD Subsystem*					
VHP-TURB	171.57	164.66	6.91	0.48	95.97	BGS Filter	41.39	40.83	0.56	0.04	98.65
VHP-TRB2	40.30	38.09	2.21	0.15	94.52	ID-FAN	37.91	34.43	3.48	0.24	90.82
HP-TURB	29.91	28.53	1.38	0.10	95.39	Desulphurizer	42.62	36.95	5.67	0.40	86.70
IP-TURB	76.97	72.11	4.86	0.34	93.69	*MEA-Based CO_2 Capture Subsystem*					
LP1-TURB	82.34	81.30	1.04	0.07	98.74	FG-Cooler	70.19	36.82	33.37	2.33	52.46
LP-TURB2	56.66	55.95	0.71	0.05	98.75	BLOWER	50.08	20.06	30.02	2.10	40.06
LP-TURB3	35.63	35.22	0.41	0.03	98.85	ABSRBR	96.2	41.52	54.68	3.82	44.55
LP-TURB4	23.77	20.74	3.03	0.21	87.25	DESRBR	235.64	153.57	82.07	5.74	65.17
BFP-TRB	20.03	15.76	4.27	0.30	78.68	PUMP	11.89	11.63	0.26	0.02	97.81
COND	26.99	0.35	26.64	1.86	1.30	T-COOLER	36.82	30.89	5.93	0.41	83.89
BF-PUMP	17.84	15.79	2.05	0.14	88.51	MHEX	48.81	36.83	11.98	0.84	75.46
						Loss (MEA)			5.15	0.36	

3.2 Advanced Exergy Analysis

Conventional exergy analysis cannot determine the interaction among components or the true potential for the improvement of each component [45]. However, an advanced exergy analysis evaluates the interaction among components, and the real potential for improving a system component/the overall system [46]. It involves splitting the exergy destruction in system components into endogenous/exogenous and avoidable/unavoidable parts [45]. It is capable of providing extra information to the conventional analysis for design improvement and operation of the SCPP with CO_2 capture systems. Therefore, advanced exergy analysis was applied to reveal the sources (endogenous/exogenous) and the potential for reduction (avoidable/unavoidable) of exergy destruction [45].

Endogenous exergy destruction ($\dot{E}_{D,n}^{en}$) is the part of exergy destruction within a component obtained when all other components operate in ideal/reversible condition and the component being considered operates with the same efficiency as in the real system [42, 47]. The *Exogenous* part of the variable ($\dot{E}_{D,n}^{ex}$) is the difference between the value of the variable within the component in the real system and the endogenous part.
Thus;

$$\dot{E}_{D,n} = \dot{E}_{D,n}^{en} + \dot{E}_{D,n}^{ex} \qquad (6)$$

The unavoidable exergy destruction ($\dot{E}_{D,n}^{un}$) [47] cannot be further reduced or eliminated due to technological limitations such as availability and cost of materials and manufacturing methods. The avoidable part ($\dot{E}_{D,n}^{av}$) is the difference between the total and the unavoidable exergy destruction. For a component, the avoidable exergy destruction is the pat that should be considered during the improvement procedure:

$$\dot{E}_{D,n} = \dot{E}_{D,n}^{un} + \dot{E}_{D,n}^{av} \qquad (7)$$

3.2.1 Splitting the exergy destruction into unavoidable/avoidable or endogenous/exogenous parts

Combining the two splitting options for exergy destruction provides the opportunity to estimate: (i) the avoidable endogenous exergy destruction ($\dot{E}_{D,n}^{av,en}$) which can be reduced by improving the design of the n^{th} component of the SCPP system from exergetic view point; (ii) the avoidable exogenous exergy destruction ($\dot{E}_{D,n}^{av,ex}$) that can be reduced by structural improvement of the overall SCPP system; (iii) unavoidable endogenous ($\dot{E}_{D,n}^{un,en}$) part; and (iv) the unavoidable exogenous part ($\dot{E}_{D,n}^{un,ex}$). Figure 6 shows the options available for splitting the exergy destruction in the n^{th} component of a system.

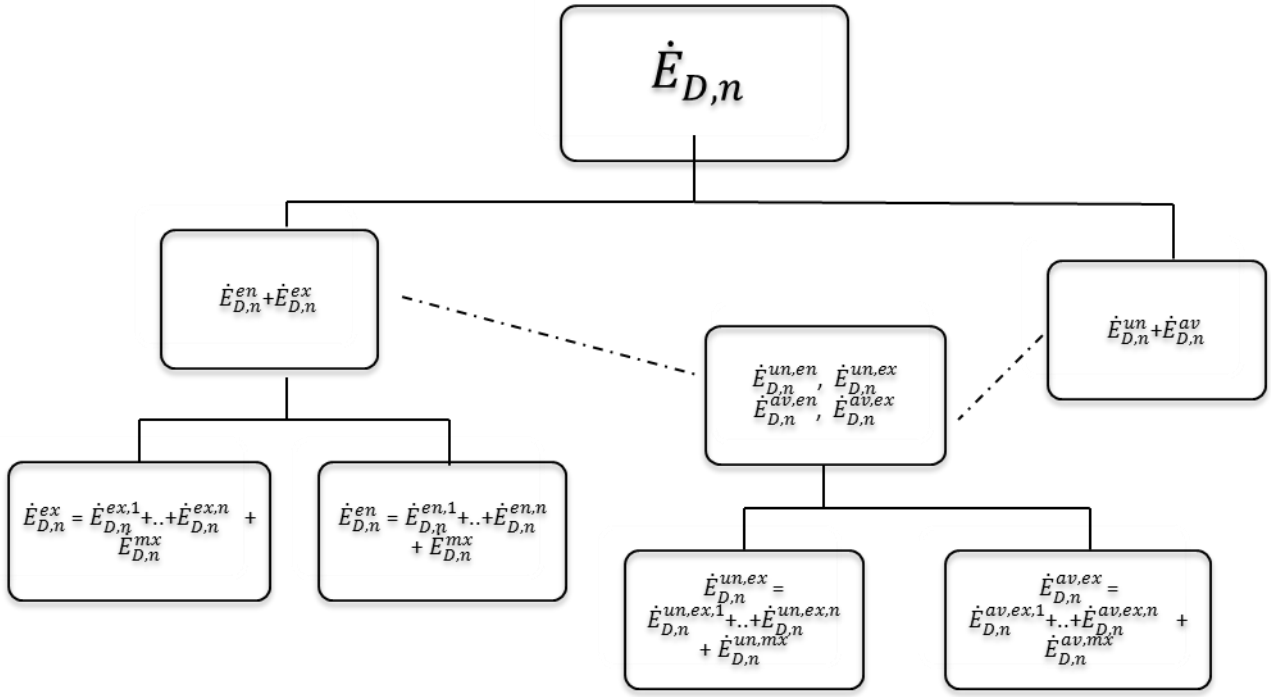

Figure 6: splitting the exergy destruction in an advanced exergy analysis. *Adapted from* [46]

These four splitting combinations can be estimated thus [3]:

$$\dot{E}_{P,n}^{un} = \dot{E}_{P,total}^{R}(\dot{E}_{D,n}/\dot{E}_{P,n})^{un} \quad (8)$$

$$\dot{E}_{D,n}^{un,en} = \dot{E}_{P,n}^{en}(\dot{E}_{D,n}/\dot{E}_{P,n})^{un} \quad (9)$$

$$\dot{E}_{D,n}^{un,ex} = \dot{E}_{D,n}^{un} - \dot{E}_{D,n}^{un,en} \quad (10)$$

$$\dot{E}_{D,n}^{av,en} = \dot{E}_{D,n}^{en} - \dot{E}_{D,n}^{un,en} \quad (11)$$

$$\dot{E}_{D,n}^{av,ex} = \dot{E}_{D,n}^{ex} - \dot{E}_{D,n}^{un,ex} \quad (12)$$

The ratio $(\dot{E}_{D,n}/\dot{E}_{P,n})^{un}$,$\dot{E}_{P,n}^{en}$, and $\dot{E}_{P,n}^{en}$ are first determined from the unavoidable and theoretical processes.

Splitting the exogenous exergy destruction within the n^{th} component into influences coming from the other components i.e. m^{th} components ($\dot{E}_{D,n}^{ex,m}$) shows the effect that the irreversibility within the m^{th} component has on the exergy destruction within the n^{th} component [46]. The variable, total avoidable exergy destruction ($\dot{E}_{D,n}^{av,total}$) is used to summarise the data obtained from the splitting of the exergy destruction [48]. This variable represents the sum of the avoidable endogenous exergy destruction within the *n*th component and the avoidable exogenous exergy destructions within the remaining components (m^{th} components) due to the n^{th} component [46]. It is used to determine the importance of the n^{th} component of any energy system from the perspective of thermodynamics.

$$\dot{E}_{D,n}^{av,total} = \dot{E}_{D,n}^{av,en} - \sum_{\substack{m=1 \\ m\neq n}}^{i} \dot{E}_{D,n}^{av,\ ex,n} \quad (13)$$

3.2.2 Conditions/Assumptions for splitting Exergy Destruction

The assumption for theoretical (TH) conditions for different components is: $\dot{E}_D = 0$ or $\dot{E}_D = min$. For turbines, fan and pump, the isentropic efficiency (η_{isent}) and mechanical efficiency (η_{mech}) should be 100%. As for single heat exchanger, both pressure drops (ΔP) and minimum temperature

difference at the pinch point (ΔT_{min}) should equal zero. The heat exchangers in the boiler subsystem are rather complicated, because the theoretical operation of a concurrent heat exchanger may affect its succeeding heat exchangers since the temperature of the steam out of the heat exchanger working theoretically may exceed the allowed temperature of its following component (i.e. turbine) or the temperature of the flue gas entering its successive heat exchanger may be below the corresponding steam temperature [3]. This problem is solved with the use of one reversible adiabatic heater (RAH) added before each heat exchanger (Figure 7) and the target of each heater is set to heat the working fluid to a specified temperature [3, 49]. The RAHs are taken offline under real process condition. In this way, the calculation of one heat exchanger starts from computing the heat absorbed by the steam and then the temperature of the flue gas entering the heater can be obtained with the pre-calculated mass flow rate of the flue gas from the heat balance.

For the unavoidable conditions (UN), the best performance characteristics can be derived with investment-efficiency considerations or based on the understanding and practical experience of the designer [3]. In this study, the unavoidable conditions are selected arbitrarily based on limitations of technology such as the isentropic efficiency (η_{isent}) of between 96-98%, and mechanical efficiency (η_{mech}) of 100% for the turbines, fan and pump. For the heat exchanger, the minimum approach temperature difference (ΔT_{min}) should not be equal to zero but based on the limitations of technology [3, 45].

For simplification purposes, the combustion process (i.e. DECOMP and BURN units in Figure 2) is considered as one separate component (FURNACE), SSH-1 & SSH-2, PSH-1 & PSH-2 are also regarded as a single component each (SSH and PSH respectively) because these two concurrent heat exchangers are arranged sequentially along the flue gas as shown in Figure 7. The simulations for fuel-savings potentials and advanced exergy analysis are conducted with the help of Aspen Plus® for individual stream exergies and Ms-Excel worksheet is used for the computations.

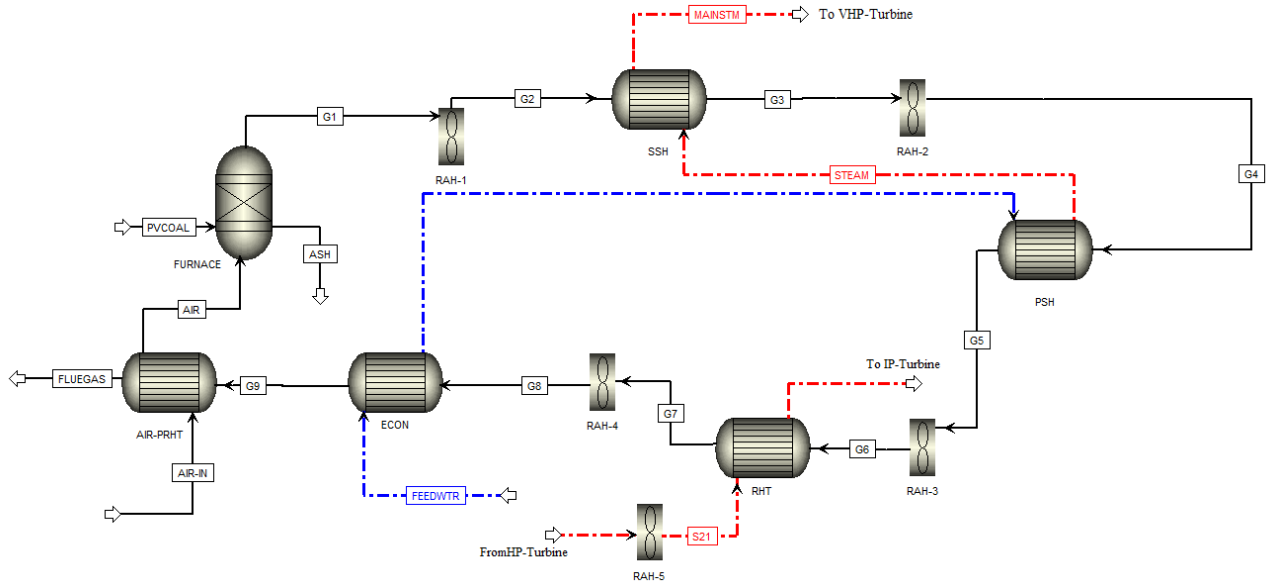

Figure 7: Once-through boiler subsystem for advanced exergy analysis

3.2.3 Fuel saving potential through individual component improvement

The contribution of irreversibilities in different components to the fuel consumptions varies significantly due to the relative position of a component to the final product [3]. The best possible

condition of a component can be regarded as the so-called "theoretical" condition within the limits of thermodynamic principles. Hence, the energy-savings potential due to an individual component ($\Delta E^{*,n}_{F,total}$) can be estimated thus [3]:

$$\Delta E^{*,n}_{F,total} = E^{R,n}_{F,total} - E^{T,n}_{F,total} \qquad (13)$$

where $E^{R,n}_{F,total}$ represents the fuel exergy consumption of the overall system when all components are under their "Real" process condition, while $E^{T,n}_{F,total}$ represents an hybrid process of the *nth* component, in which only the component of interest operates theoretically while all the other components operates at their real process conditions.

4 Results and Discussion

4.1 Conventional Exergetic Performance Analyses

4.1.1 Boiler subsystems

Table 6 contains the results obtained from the conventional exergy analysis of the whole SCPP system with CO_2 capture. It can be seen from Table 6 that the boiler section has the highest exergy destruction with the BURN and DECOMP units where the combustion of fuel take places accounts for the highest irreversibility in the boiler and hence a low exergy efficiency (68%). It accounts for about a third of the total fuel exergy destroyed. Table 6 also shows that the thermodynamic inefficiencies of heat exchangers especially the radiant superheaters (SSHs) are generally higher than those of convective heat exchangers in the flue gas duct. While in the convective heat exchangers, the heat release from hot side to cold side is lower than the in the radiation, and the temperature difference for heat transfer is lower. Hence, the exergy efficiencies of the radiant heat exchangers (SSH-1 and SSH-2) are usually lower than 80%. Because the flue gas temperature decreases rapidly in radiation sections, the convection sections always have relatively high efficiency.

4.1.2 Turbine subsystem

Unlike the once-through boiler, the turbines performed better with exergy efficiency in the range of 95%-99% for HP and IP turbines, while the LP turbines show a decrease in efficiency from the 98% to about 79% from the first stage to the last due to the state of the working fluid being a wet steam (Table 6). The low efficiency is mainly due to the losses associated with the wet steam and speed loss of the last stage of the turbine.

4.1.3 Feedwater heating subsystem

Table 6 also shows the exergetic performances of regenerative feedwater heaters improve steadily along the direction of flow of water. Two main factors that determine the exergy performance of feedwater heaters are (i) the increase in temperature of the cold fluid, and (ii) the temperature difference for heat transfer. This is mainly because the higher the cold fluid temperature, the lower the exergy destroyed (i.e. higher exergy efficiency). However, deviations from the main trend are sometimes encountered due to large temperature difference of the condensate section or the high temperature steam extraction after the reheating process [3].

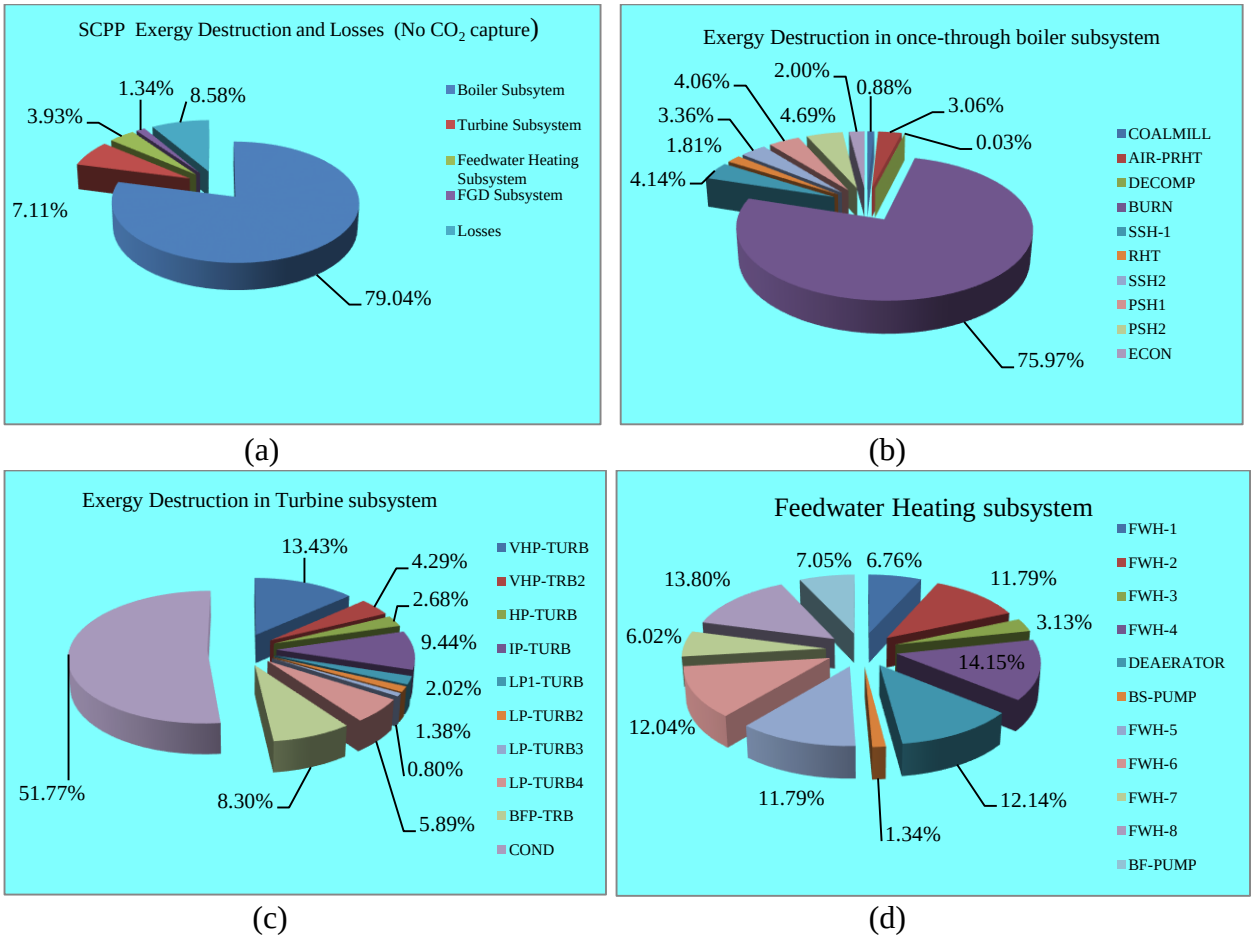

Figure 8 Distribution of Exergy losses and Destruction in the SCPP Subsystems

4.1.4 Location of Exergy Destruction and Losses

Figure 8 shows the location and the distribution of exergy destruction and losses (%) associated with the SCPP system without CO_2 capture. It is evident from Figure 8(a) that the exergy destruction within the once-through boiler subsystem (79%) dominates the overall exergy dissipation, followed by the total exergy losses in the SCPP process (about 9%), and the turbine subsystem (over 7%). Hence, largest energy-savings potential may be present in the boiler subsystem. Figure 8(b) shows the spatial distribution of exergy destruction in the boiler subsystem. The boiler combustion zone "BURN" and "DECOMP" units (about 76% and 5% respectively) and the radiant superheaters (about 6%) contributes the largest proportion of exergy destruction, the convective superheaters (0.03% and 4% respectively) and the economiser (2%) have much lower contributions. However, the effective application of the enormous amount of exergy of waste flue gas should be further investigated for the further reduction of fuel consumption. Figure 8(c) shows that the largest proportion (about 52%) of exergy destruction within the turbine subsystem comes from the condenser (i.e. a total of 3.7% destruction in the SCPP accounted for in the condenser) ; and the turbines stages combined (about 48%) accounts for the remainder (about 3.4% of exergy destroyed in the SCPP system). Figure 8(d) illustrates the exergy destruction within the feedwater heaters subsystem. In summary, from conventional exergy analysis of the whole SCPP, around 60% of exergy destroyed was in the furnace.

4.1.5 CO_2 Capture subsystem

Table 6 also shows the exergy destruction and efficiency of the FGD unit and the MEA capture system integrated with SCPP system. Figure 9(a) and (b) illustrates spatial distribution of the exergy destruction in these systems respectively. The results reveal that the absorber (26%) and the desorber (36%) are the main sources of exergy destruction. The feed cooler (18%) and the blower (16.5%) are also contributing strongly. The total exergy destruction is about 203 MW (1.58 MJ/kg CO_2.). Process equipment such as the pump, the blower and the solvent cooler are minor contributors to the exergy destruction. The exergy loss due to the consumption of MEA was included in the overall exergy destruction. Using the chemical exergy of MEA in the liquid phase of 1536 kJ/mol [16], an exergy loss of 5.15MW (0.04 MJ/kg CO_2) amounting to about 2.3 % of total exergy destroyed in the CO_2 capture subsystem.

Too much Exergy destruction in an individual component (e.g. desorber) of a system should be avoided in order to prevent large local driving force which is unfavourable for total loss of exergy minimization [16]. This can be achieved by integrating heat and mass transport in the absorber and desorber as discussed in the case studies in section 4.2. However, lower driving force means a larger area for mass transfer and increased capital cost for internals. Dealing with this two opposing factors will require an economic analysis of the trade-offs for optimal design. It should be noted that the CO_2 compression system is an obvious additional source of exergy loss which is not considered in this study.

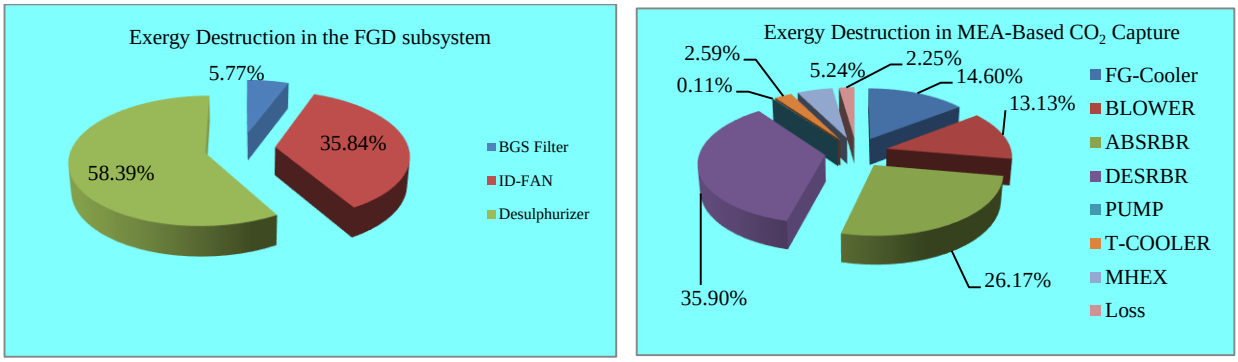

(a) (b)

Figure 9 Distribution of Exergy Destruction in (a) FGD and (b) CO_2 Capture subsystems

4.2 Reducing exergy destruction/losses in MEA-Based CO_2 Capture: Case Study

Analysis of the energy consumption of the CO_2 capture system and the overall exergy destruction in the integrated system necessitated the development of several variations of the conventional CO_2 capture [19, 27]. In this study, three cases were considered, which include the following:

- Case 1: SCPP with AIC
- Case 2: SCPP with SF
- Case 3: SCPP with AIC + SF

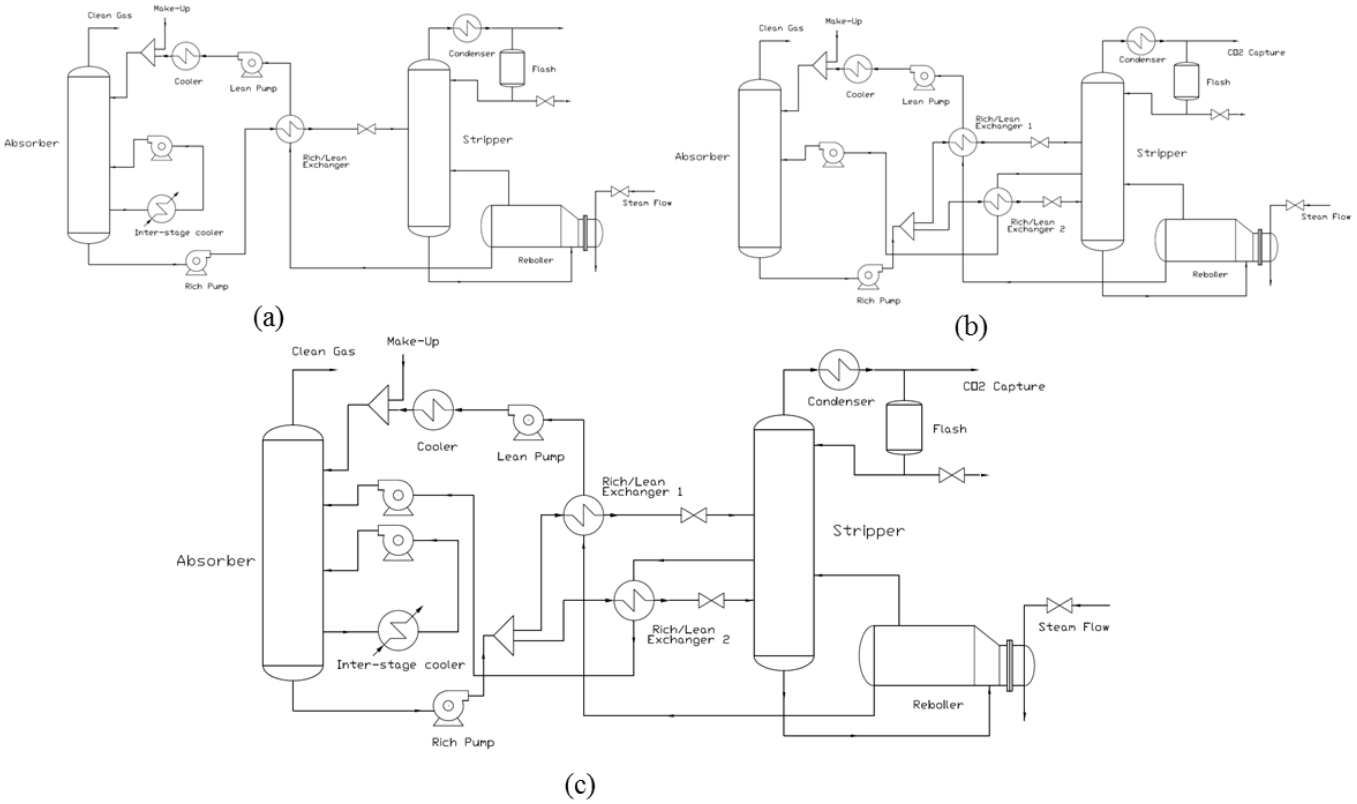

Figure 10 CO_2 Capture Scenarios integrated with SCPP: (a) AIC (b) SF (c) AIC+SF

4.2.1 SCPP-AIC configuration

The inclusion of intermediate cooler in the absorber (AIC) counteracts the temperature increase in the liquid stream due to the release of heat of reaction. The aim of the AIC modification to the conventional system as shown in Figure 10(a) was to extract a semi-rich stream from the lower part of the absorber, cool it to 25 ◦C and recycle back to the absorber column. All other components in the system were identical to the base case. Sensitivity analysis was performed on a standalone configuration of AIC to efficiently estimate the flow rate and the location of the side-stream which was withdrawn for intercooling to achieve lower reboiler duty compared to the Base case. Table 8 shows a summary of the system performance with the integrated AIC approach. The result shows about 0.2% reduction in exergy destruction when compared to the SCPP system with base case CO_2 capture. The reboiler duty, energy penalty and the efficiency penalty were decreased by about 3.2%, 0.43% and 0.16%respectively. The exergetic efficiency of the AIC-integrated system was also improved by about 0.5% when compared to the base case. Figure 11(b) shows the spatial distribution of exergy destruction in SCPP-AIC system.

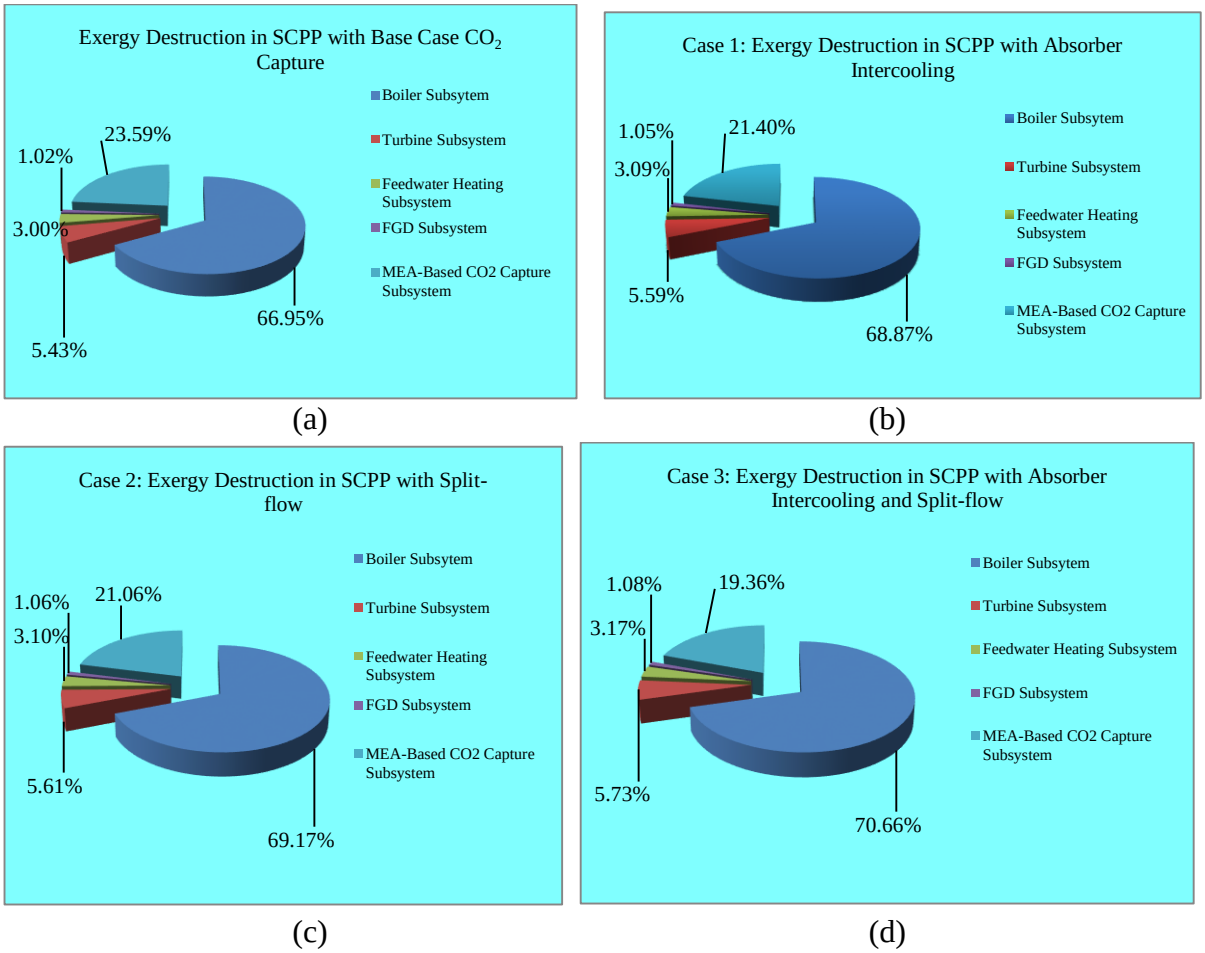

Figure 11 Exergy Destruction in SCPP with three cases of MEA-Based CO_2 Capture

4.2.2 SCPP-SF configuration

The SF configuration for chemical absorption processes (Figure 10b) is based on the concept of thermodynamic principles of reducing the driving forces to reduce steam consumption for solvent regeneration. This modification make the driving forces more uniform and can simultaneously reduce both exergy losses and capital investments [27, 43]. In the SCPP-SF configuration, instead of single rich amine feed stream to the stripper column there are split-flows; a part of the cold rich amine solvent is fed to the stripper top without passing through the lean/rich heat exchanger, thereby directly cooling off the stripper top. This results in a reduction in the heat exchanger duty as a result of decrease in the cold-side flow rate. The idea is to approach the theoretical level of adding and removing all flow streams which causes more evenly distribution of driving forces (mass transfer core) through the vapour and liquid phase [27]. The result shows about 0.5% reduction in exergy destruction when compared to the SCPP system with base case CO_2 capture. The reboiler duty, energy penalty and the efficiency penalty were decreased by about 7%, 1.41% and 0.6% respectively. The exergetic efficiency of the SCPP-SF integrated system was also improved by about 1.1% when compared to the base case. Figure 11(c) shows the spatial distribution of exergy destruction in SCPP-AIC system.

4.2.3 SCPP-(AIC+SF) Configuration

This *AIC+SF* configuration illustrated in Figure 10(c) combined the effect of AIC and the SF configuration. Table 8 shows a summary of the system performance. The result shows about 3.1% reduction in exergy destruction when compared to the SCPP system with base case CO_2 capture. The reboiler duty, energy penalty and the efficiency penalty were decreased by about 16%, 2.8% and 1.1% respectively. The exergetic efficiency of the SCPP-SF integrated system was also improved by about 4.5% when compared to the base case. Figure 11(d) illustrates the spatial distribution of exergy destruction in SCPP-(AIC+SF). Table 7 shows a summary of the performance of the CO2 capture scenarios investigated.

Table 7 System Performance Indicator of the SCPP with the CO_2 Capture Scenarios

Description	Reference SCPP	SCPP + PCC Base Case	SCPP + PCC Case 1	SCPP + PCC Case 2	SCPP + PCC Case 3
Performance Summary					
Total (steam turbine) power (MWe)	580.26	482.28	484.52	486.42	488.58
Auxiliary load (MW)	28.28	52.04	51.95	48.45	42.8
Gross plant power (MW)	551.98	430.24	432.57	437.97	445.78
Generator loss (MW)	1.83	1.83	1.83	1.83	1.83
Net power output (MWe)	550.15	428.41	430.74	436.14	443.95
Unit efficiency, HHV (%)	39.10	30.45	30.61	31.00	31.55
CO_2 Capture Performance Summary					
Reboiler Duty (MW)	-	528.78	511.81	492.02	466.57
Energy penalty (%)	-	22.13	21.70	20.72	19.30
Efficiency penalty (%)	-	8.65	8.49	8.10	7.55
Exergetic Performance					
Exergy Destruction, y_D (%)	52.61	46.27	46.15	45.81	43.19
Exergy Losses, E_L (%)	8.34	5.03	4.62	4.37	3.58
Exergetic efficiency, Ɛ (%)	39.05	48.7	49.23	49.82	53.23

4.3 Advanced Exergetic Performance Analysis

4.3.1 Fuel Savings Potential

Table 8 present the fuel-saving potentials ($\Delta E^{*,n}_{F,\ tot}$) of the overall SCPP system based on the control volumes shown in Figures 1 to Figure 4. The fuel saving potential was evaluated by improving each component in isolation. The total fuel-saving potential due to improvement in the once-through boiler subsystem (about 61 MW) is very low compared to the turbine system (104 MW). This is because the main steam and the reheat steam flow are determined by the turbine subsystem which in turns implies that the heat absorbed in the boiler is fixed, given its conditions. Hence, at constant air/fuel ratio ($\alpha_{airfuel}$) and furnace exit gas temperature there will be only a limited potential to reduce fuel consumption from the boiler subsystem. In this case, only by reducing the pressure drops of working fluid can the fuel consumption be reduced. Table 8 also shows that fuel consumption can be reduced by 55 MW from the theoretical operations of the air preheater (AIR-PRHT) and the combustion chamber (FURN). Thus, the promising approaches for reducing fuel consumption from the design perspective of the boiler subsystem would be by reducing the air/fuel

ratio ($\alpha_{airfuel}$) and the furnace exit gas temperature. For the turbine subsystem, the improvements of the turbines, the feed pumps, feed pump turbines, and the generator are of great significance for reducing fuel consumption, although their exergy destructions under real processes are much smaller than those of the boiler subsystem. The benefits obtained from the turbine subsystem are almost double that of the boiler subsystem. Also, the performance of individual regenerative feedwater heater almost has no influence on fuel consumption in this case, since the pressures of steam extractions remain the same.

4.3.2 Avoidable /Unavoidable Endogenous/Exogenous exergy destruction

Table 8 shows that majority of the exergy destruction within all SCPP components is endogenous However, the ratio of the exogenous part of the exergy destruction differs considerably from components to components. For the boiler subsystem, about 20% of the overall exergy destroyed within it is exogenous as shown in Figure 12(b). The results shown in Figure 13(b) reveal that about 14% of the exergy destructions in the turbine subsystem are exogenous. In the regenerative feedwater heating subsystem, about 30% of exergy destroyed within it is exogenous as shown in Figure 14(b). The components in the boiler subsystem have large absolute exogenous exergy destruction of about 87MW (Figure12). Hence, their performances are significantly affected by the exergy destructions in the components of the turbine subsystem. The real potential for improving a component is not fully revealed by its total exergy destruction but by its avoidable part [3]. Table 8 also show that a significant part (40–49%) of the exergy destruction within PSH, RHT and AIR-PRT is avoidable. It also shows that due to combustion reactions, most of the exergy destruction (331 MW) within combustion chamber (FURN) is unavoidable in comparison with the avoidable part (30 MW). Also, about 20% of the exergy destruction within SSH (about 17%) and ECON (19%) can be avoided. For the turbine subsystem, about 30–50% of exergy destruction can be avoided as shown in Figure 13(a). Figure 14(a) also illustrates that the avoidable parts of the exergy destruction in the feedwater heating subsystem is about 24%. Since the work is pure exergy and a slight change of the efficiency of turbine subsystems contributes largely to fuel consumption improvement, more attention should be directed toward the improvement of the efficiencies of turbines, pumps and fans. Most of the avoidable exergy destructions within the heat exchangers in the boiler subsystems (75%), turbine stages (92%) are endogenous as shown in Figures 12(c) and 13(c) respectively; hence, the improvement measures for these components should be concentrated on the components themselves. The combustion process has an avoidable-exogenous exergy destruction of about 18MW and, thus, its performance improvement should also consider the reductions of exergy destruction of other components. Figure 14(c) also reveals that the exogenous exergy destruction contributes over 70% of the avoidable part within the feedwater heating subsystem. Hence, improving feedwater heaters can be more efficiently achieved at the subsystem level. It is important to note that there are no contradictions between the discussions of the fuel-savings potentials in section 4.3.1 and the advanced exergy analysis in section 4.3.2 as pointed out by [3]. The former focuses on the influence of each component on the overall fuel consumption, while the latter is based on the energy savings potential of the considered component itself.

Table 8 Selected results of the Fuel saving potential and advanced exergy analysis of SCPP subsystems

Components	$E^{T,n}{}_{F,tot}$	$\Delta E^{*,n}{}_{F,tot}$	$E^{T}{}_{D,n}$	$E^{R}{}_{D,n}$	$E^{un}{}_{D,n}$	$E^{av}{}_{D,n}$	$E^{en}{}_{D,n}$	$E^{ex}{}_{D,n}$	$E^{en}{}_{D,n}$		$E^{ex}{}_{D,n}$	
									$E^{un,en}{}_{D,n}$	$E^{av,en}{}_{D,n}$	$E^{av,ex}{}_{D,n}$	$E^{un,ex}{}_{D,n}$
Boiler subsytem												
FURN	1390.37	17.35	361.50	361.50	330.95	30.55	304.45	57.05	291.66	12.79	17.76	39.29
AIR-PRT	1371.03	36.68	6.81	18.00	9.24	8.76	16.15	1.85	8.25	7.90	0.86	0.99
SSH	1404.17	3.55	149.67	203.17	169.59	33.58	181.59	21.58	150.54	31.05	2.53	19.05
PSH	1407.10	0.62	2.89	13.80	7.59	6.21	12.24	1.56	6.79	5.45	0.76	0.80
RHT	1404.91	2.81	4.28	24.25	14.28	9.97	21.58	2.67	12.58	9.00	0.97	1.70
ECON	1407.50	0.22	6.20	13.42	10.74	2.68	11.64	1.78	9.30	2.34	0.34	1.44
Turbine subsystem												
VHP-TURB	1386.47	21.25	0.00	7.11	6.18	0.93	6.46	0.65	5.61	0.85	0.08	0.57
VHP-TRB2	1400.94	6.78	0.00	2.27	1.58	0.69	1.59	0.68	0.99	0.60	0.09	0.59
HP-TURB	1401.10	6.62	0.00	1.42	0.79	0.63	1.16	0.26	0.54	0.62	0.01	0.29
IP-TURB	1399.30	8.42	0.00	4.81	3.24	1.57	3.18	1.63	1.73	1.45	0.12	1.51
LP1-TURB	1401.19	6.53	0.00	1.01	0.65	0.36	0.92	0.09	0.57	0.35	0.01	0.08
LP-TURB2	1402.74	4.98	0.00	0.68	0.39	0.29	0.61	0.07	0.33	0.28	0.01	0.06
LP-TURB3	1402.25	5.47	0.00	0.53	0.37	0.16	0.48	0.05	0.36	0.12	0.04	0.01
LP-TURB4	1382.22	25.50	0.00	3.64	1.82	1.82	3.32	0.32	1.65	1.67	0.15	0.17
BFP-TRB	1389.80	17.92	0.00	2.10	1.38	0.72	1.18	0.92	0.61	0.57	0.15	0.77
COND	1407.72	0.00	31.68	31.68	0.00	31.68	25.54	6.14	-	-	-	-
Feedwater heating subsystem												
FWH-1	1407.11	0.61	1.94	2.03	1.74	0.29	1.79	0.24	1.55	0.24	0.05	0.19
FWH-2	1407.13	0.59	3.26	3.41	2.93	0.48	2.48	0.93	2.40	0.08	0.40	0.53
FWH-3	1406.73	0.99	0.86	0.93	0.76	0.17	0.64	0.29	0.60	0.04	0.13	0.16
FWH-4	1405.92	1.80	4.00	4.03	3.58	0.45	2.94	1.09	2.93	0.01	0.44	0.65
DEAERATOR	1406.98	0.74	3.12	2.98	2.64	0.34	1.86	1.12	1.80	0.06	0.28	0.84
BS-PUMP	1407.42	0.30	0.00	2.31	1.39	0.92	1.40	0.91	0.93	0.47	0.45	0.46

FWH-5	1406.14	1.58	2.86	2.90	2.58	0.32	2.26	0.64	2.14	0.12	0.20	0.44
FWH-6	1406.65	1.07	2.18	2.45	2.14	0.31	1.62	0.83	1.59	0.03	0.28	0.55
BF-PUMP	1402.38	5.34	0.00	2.17	1.16	1.01	1.58	0.59	0.85	0.73	0.28	0.31
FWH-7	1405.92	1.80	1.64	2.19	1.89	0.30	1.66	0.53	1.59	0.07	0.23	0.30
FWH-8	1405.07	2.65	4.03	4.65	3.28	1.37	2.85	1.80	1.87	0.98	0.39	1.41
FGD Subsystem												
BGS Filter	1407.25	0.47	0.38	0.62	0.41	0.21	0.56	0.06	0.48	0.08	0.13	-0.07
ID-FAN	1405.90	1.82	0.00	4.21	2.86	1.35	3.67	0.54	2.87	0.80	0.55	-0.01
Desulphurizer	1403.98	3.74	2.86	5.81	4.63	1.18	4.43	1.38	2.96	1.47	-0.29	1.67

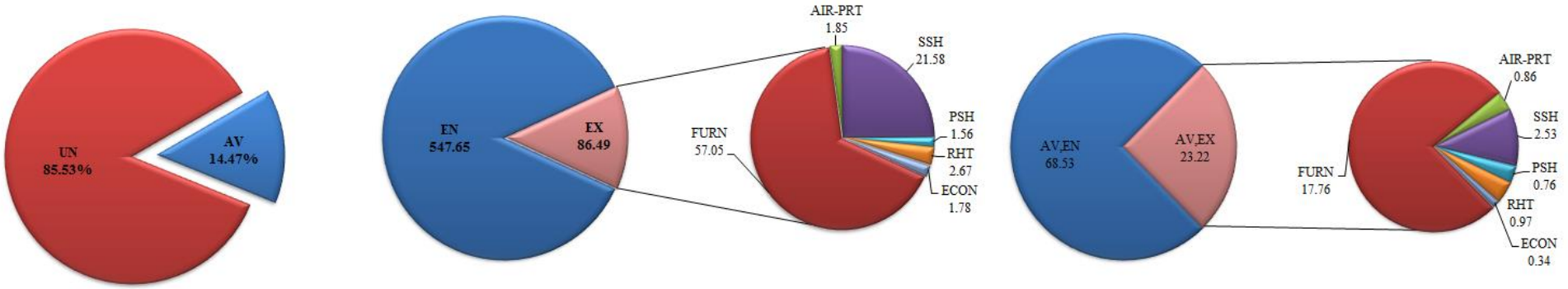

(a) (b) (c)

Figure 12 Advanced exergy Analysis of boiler subsystem into (a) AV/UN (b) EN and EX (c) AV, EN and UN, EN

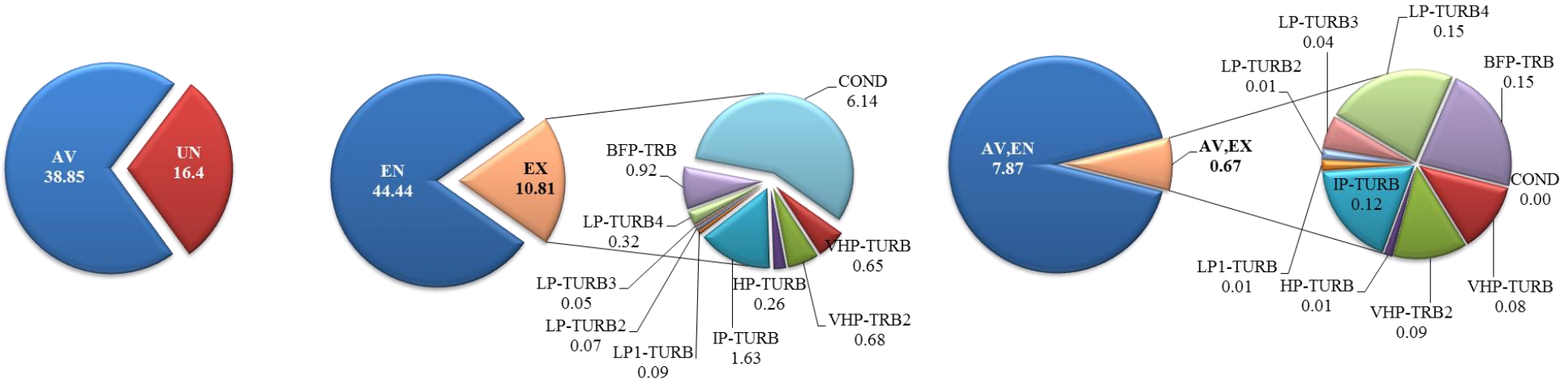

(a) (b) (c)

Figure 13 Advanced exergy Analysis of turbine subsystem into (a) AV/UN (b) EN and EX (c) AV,EN and UN,EN

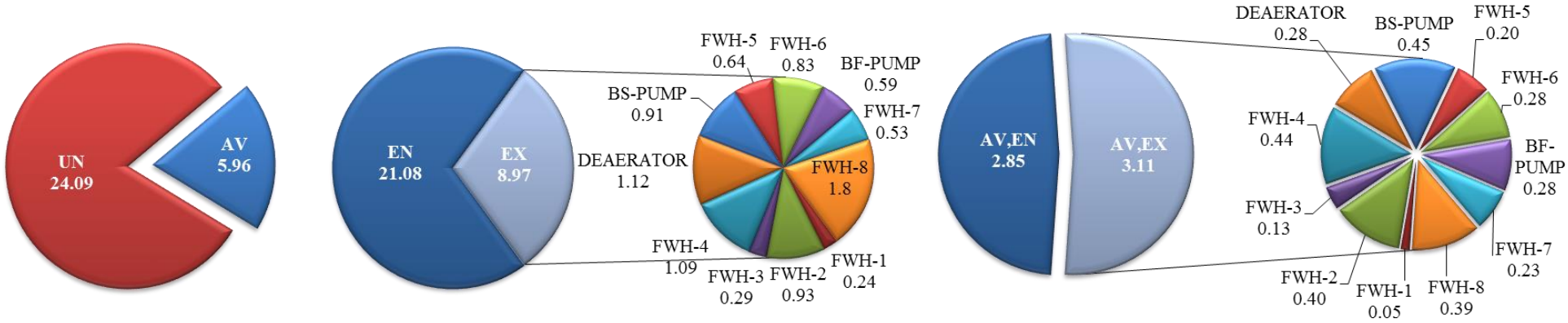

(a) (b) (c)

Figure 14 Advanced exergy Analysis of feedwater subsystem into (a) AV/UN (b) EN and EX (c) AV, EN and UN, EN

5 Conclusion

The conventional and advanced exergetic analysis performed in this paper allows a consistent and detailed evaluation of energy consumption in the SCPP integrated with CO_2 capture from the thermodynamic point of view. The conventional exergy analysis evaluates the exergy destruction with the whole system. The study also investigates the improvement of energy penalties and reduction of exergy destruction in the CO_2 capture subsystem. Four cases of the integrated system were considered for reducing exergy destruction in the system by reducing the driving forces in the CO_2 capture process: conventional process, SCPP-AIC, SCPP-SF, and SCPP-(AIC+SF). The AIC+SF configuration shows the most significant reduction in exergy destructed when compared to the SCPP system with conventional CO_2 capture. The advanced exergetic analysis is based on a splitting of exergy destruction into many parts, in order to estimate (i) the real potential for improving the components, and (ii) the interconnections between the components. The boiler subsystem has the largest exergy destruction but also has a limited influence on fuel-saving potentials of the system. The turbine subsystem shows very small exergy destruction compared to the boiler subsystem, but more significance in reducing fuel consumption. This study show that a combination of improvement in turbine performance design and reduction of the driving forces responsible for the CO_2 capture (without compromising cost) can help improve the rational efficiency of the integrated system.

REFERENCES

[1] Freund P. (2003), Making deep reductions in CO_2 emissions from coal-fired power plant using capture and storage of CO_2. Proc Inst. Mech Eng Part A: J Power Energy 217:18.

[2] Wang M, Lawal A., Stephenson P., Sidders J., Ramshaw C. (2011), Post-combustion CO_2 capture with chemical absorption: A state-of-the-art review, *Chemical Engineering Research and Design*, vol. 89, pp.1609–1624.

[3] Yang Y., Wang L., Dong C., Xu G., Morosuk T., Tsatsaronis G. (2013), Comprehensive exergy-based evaluation and parametric study of a coal-fired ultra-supercritical power plant, Applied Energy 112, 1087-1099.

[4] Chalmers H, Gibbins J. (2007), Initial evaluation of the impact of post-combustion capture of carbon dioxide on supercritical pulverised coal power plant part load performance, *Fuel*, vol. 86, pp. 2109–2123.

[5] Senguptal S., Datta A., Duttagupta S. (2007), Exergy analysis of a coal-based 210MW thermal power plant, *Int. J. Energy Res*, 31:14-28.

[6] Kotas T.J. The Exergy Method of Thermal Plant Analysis. Kriegler Publishing Company: Malabar, Florida, 1995.

[7] Szargut J. Exergy method: technical and ecological applications. Southampton, UK: WIT; 2005.

[8] Horlock, J.H., Young, J.B., Manfrida, G., (2000), Exergy Analysis of Modern Fossil–Fuel Power Plants, *J. Eng. Gas Turbines and Power*, Vol. 122, 1-7.

[9] Dincer I, Al-Muslim H. Thermodynamic analysis of reheats cycle steam power plants. *International Journal of Energy Research* 2001; 25:727–739.

[10] Reddy V.S., Kaushik S.C., Tyagi S.K. (2014), Exergetic analysis and evaluation of coal-fired supercritical thermal power plant and natural gas-fired combined cycle power plant, *Clean Techn Environ Policy 16:489-499.*

[11] Ameri M., Ahmadi P., Hamidi A. (2009), Energy, exergy and exergoeconomic analysis of steam power plant: A case study, *Int. J. Energy Res., 33:449-512.*

[12] Siamak F., Saffar-Avval M., Younessi-Sinaki M. (2008), Efficient design of feedwater heaters network in steam power plants using pinch technology and exergy analysis, *Int. J. Energy Res., 32:1-11.*

[13] Srinivas T. (2009), Study of a deaerator location in triple-pressure reheat combined power cycle. *Energy 34:1364–1371.*

[14] Reddy B.V., Mohamed K. (2007), Exergy analysis of natural gas fired combined cycle power generation unit, *Int. J. Exergy 4:180–196.*

[15] Woudstra N., Woudstra T., Pirone A., Van Der Stelt T. (2010), Thermodynamic evaluation of combined cycle plants, *Energy Conv. Mgt. 51:1099-1110.*

[16] Geuzebroek, F.H., Schneiders, L.H.J.M., Kraaijveld, G.J.C., Feron, P.H.M. (2004), Exergy analysis of alkanolamine—based CO_2 removal unit with Aspen Plus, *Energy 29 (9/10): 1241–1248.*

[17] Valenti, G., Bonalumi, D., Macchi, E. (2009). Energy and exergy analyses for the carbon capture with the Chilled Ammonia Process (CAP). *Energy Procedia 1: 1059–1066.*

[18] Lara Y., Martinez A., Lisbona P., Bolea I., Gonzalez A., Romeo L.M. (2011), Using second law of thermodynamics to improve CO_2 capture systems, *Energy Procedia 4:1043–1050.*

[19] Aroonwilas A., Veawab A. (2007), Integration of CO_2 capture unit using single and blended-amines into supercritical coal-fired power plants: Implications for emission and energy management. *Int. J. Greenhouse Gas Control 1 (2), 143–150.*

[20] Lucquiaud, M., and Gibbins, J., (2009), "Retrofitting CO_2 capture ready fossil plants with post-combustion capture. Part 1: requirements for supercritical pulverized coal plants using solvent-based flue gas scrubbing", vol. 223, no. Part A, pp. 213-226.

[21] Sanpasertparnich, T., Idem, R., Bolea, I., deMontigny, D., Tontiwachuwuthikul, P. (2010), Integration of post-combustion capture and storage into a pulverized coal-fired power plant, *Int. J. Greenhouse Control, 4(3): 499-510.*

[22] Zhang, D., Liu P., West, L., Li Z., Ni, W (2011) "Reducing Initial Barriers for CCS Deployment on Pulverized Coal-fired Power Plants in China by Optimizing the Capture Ratio of Carbon dioxide", *International Conference for Renewable Energy and Environment (ICMREE), 20-22 May, 2011, Shanghai, China Vol. 2, pp. 1619-1623.*

[23] Pfaff, I., Oexmann, J., Kather, A., (2010), Optimised integration of post-combustion CO_2 capture process in greenfield power plants, *Energy 35: 4030–4041.*

[24] Harkin T., Hoadley A., Hooper B. (2009), Process integration analysis of a brown coal fired power station with CO_2 capture and storage and lignite drying. *Energy Procedia, 1(1):3817–3825.*

[25] Dawid H.P., Biliyok C., Yeung H., Bialecki R. (2014), Heat integration and exergy analysis for a supercritical high-ash coal-fired power plant integrated with a post-combustion carbon capture process, Fuel 134: 126-139.

[26] Hagi H., Le Moullec Y., Nemer M., Bouallou C. (2014), Performance assessment of first generation oxy-coal power plants through an exergy-based process integration methodology, *Energy, In Press.*

[27] Amrollahi, Z., Ertesvag, I.S., Bolland, O. (2011), Optimized process configurations of post-combustion CO_2 capture for natural-gas-fired power plant—power plant -Exergy analysis, *Int. J. Greenhouse Gas Control, 5:1393-1405.*

[28] Woods M.C., Capicotto P.J., Halsbeck J.L., Kuehn N.J., Matuszewski M., Pinkerton L.L., Rutkowski M.D., Schoff R.L., Vaysman V. (2007), Bituminous Coal and Natural Gas to Electricity. In: Cost and Performance Baseline for Fossil Energy Plants, Final Report DOE/NETL-2007/1281, National Energy Technology Laboratory (NETL), USA.

[29] Zhang Y., Chen C-C. (2013), Modelling CO2 absorption and desorption by aqueous monoethanolamine solution with Aspen rate-based model, *Energy Procedia* 37:1584-1596.

[30] Hikita H, Asai S, Ishikawa H, Honda M. (1977), The kinetics of reactions of carbon dioxide with monoethanolamine, diethanolamine, and triethanolamine by a rapid mixing method, *Chem. Eng. J.*, 13:7-12.

[31] Pinsent B.R., Pearson L., Roughton F.J.W. (1956), The kinetics of combination of carbon dioxide with hydroxide ions, *Trans. Faraday Soc.*, 52:1512-1520.

[32] Mangalapally H.P., Hasse H. (2011), Pilot plant study of post-combustion carbon dioxide capture by reactive absorption: methodology, comparison of different structured packings, and comprehensive results for monoethanolamine. *Chemical Engineering Research and Design*, 89:1216-1228.

[33] Aspen Technology Inc. (2006), *Aspen properties reference manual*, Burlington, MA: Aspen Technology Inc.

[34] Fair J.R., Bravo J.L. (1987), Prediction of mass transfer efficiencies and pressure drop for structured tower packings in vapour/liquid service. *Inst. Chem. Eng. Symp. Ser.*, 104:A183-200.

[35] Bravo J.L., Rocha J.A., Fair J.R. (1992), Comprehensive model for the performance of columns containing structured packings. *Inst. Chem. Eng. Symp. Ser.*, 129:A439-457.

[36] Taylor R., Krishna R. (1993), *Multicomponent Mass Transfer*, New York: John Wiley & Sons, Inc.

[37] Sinnott R.K., Towler G.(2013), Chemical engineering design – principles, practice and economics of plant and process design. 2nd ed. Oxford, UK: Elsevier.

[38] Lawal A., Wang M., Stephenson P., Obi O. (2012), Demonstrating full-scale post combustion CO_2 capture for coal-fired power plants through dynamic modelling and simulation. Fuel 101:115–28.

[39] Sulzer, (2012). Structured packings for distillation, absorption and reactive distillation. Winterthur, Switzerland: Sulzer Chemtech Ltd.

[40] Kaushik S.C., Siva Reddy V., Tyagi S.K. (2011) Energy and exergy analysis of thermal power plants: a review. Renew Sustain Energy Rev 15:1857–1872.

[41] AspenTech. (2013), Aspen physical property system: physical property methods. Burlington, MA, USA: Aspen Technology Inc.

[42] Tsatsaronis G, Winhold M. (1984), Thermoeconomic analysis of power plants. In: Final Report EPRI AP-3651, RP 2029-8, Electric Power Research Institute (EPRI), Palo Alto, CA, USA.

[43] Leites, I.L., Sama, D.A., Lior, N., (2003). The theory and practice of energy saving in the chemical industry: some methods for reducing thermodynamic irreversibility in chemical technology processes. *Energy* 28, 55–97.

[44] Haywood R.W. (1981), Equilibrium thermodynamics for engineers and students. Chichester, New York, Brisbane, Toronto: Wiley Interscience Publication, John Wiley and Sons Inc.

[45] Wang L., Yang Y., Morosuk T., Tsatsaronis G.(2012) Advanced thermodynamic analysis and evaluation of a supercritical power plant. Energies 5(6):1850–63.

[46] Morosuk T., Tsatsaronis G., Schult M. (2013), Conventional and Advanced Exergy Analyses: Theory and Application, *Arab J. Sci. Eng* 38:395-404.

[47] Tsatsaronis, G.; Morosuk, T. (2008), A general exergy-based method for combining a cost analysis with an environmental impact analysis. In: Proceedings of the ASME International Mechanical Engineering Congress and Exposition, files IMECE2008-67218, IMECE2008-67219, Boston, Massachusetts, USA.

[48] Morosuk, T., Tsatsaronis, G. (2009), Advanced exergy analysis for chemically reacting systems—application to a simple open gas-turbine system. *Int. J. Thermodyn.* 12(3), 105–111.

[49] Morosuk T., Tsatsaronis G. (2009), Advanced exergetic evaluation of refrigeration machines using different working fluids. *Energy* 34(12):2248–58.